Damage detection of beam-like structures using wavelet transform and subtraction of intact and damaged mode shapes

Morteza Saadatmorad[1], Ramazan-Ali Jafari-Talookolaei[1*]

[1]Babol Noshirvani University of Technology, Babol, Iran
[*]Corresponding author: ramazanali@gmail.com

ARTICLE INFO	ABSTRACT
	Detecting damages with low levels presents a significant challenge in structural assessment. Many existing methods fail to detect damages or cracks below a severity threshold of 10%. Localizing on-surface damages, especially those with low levels, adds to this complexity. This study introduces a novel technique to address these issues by employing wavelet transformation on the difference between damaged and intact mode shapes. A finite element model is developed to derive the governing equations for thin beams, yielding the mode shape signals necessary for analysis. These signals are subsequently decomposed using wavelet transform. Both numerical simulations and experimental validations confirm the method's efficacy in detecting on-surface damages below the 10% level.

1. Introduction

Damage identification of a structure at the early stages plays a crucial role in maintaining its health (Azami & Salehi, 2019). Moreover, timely damage identification can save on repair costs. In recent decades, a considerable number of damage identification techniques have been proposed to assess the health of structures and identify their damages (Wahab & De Roeck, 1999). Techniques based on the vibration characteristics of structures form a broad category of these methods (Saadatmorad, Jafari-Talookolaei, Pashaei, & Khatir, 2021; Saadatmorad, Shahavi, & Gholipour, 2024). Vibration characteristics such as the natural frequencies, mode shapes, and stiffness of structures are used to identify structural damage (Khatir, Dekemele, Loccufier, Khatir, & Wahab, 2018; Saadatmorad, Jafari-Talookolaei, Pashaei, Khatir, & Wahab, 2022c). Research has confirmed that regional stiffness decreases at the damaged areas because of the damage (Bjørheim, Siriwardane, & Pavlou, 2022). Furthermore, many studies have shown that damage leads to a reduction in the natural frequencies of structures (Saadatmorad, Khatir, Le, Benaissa, & Mahmoudi, 2024). In practice, it is infeasible to evaluate the higher mode natural frequencies and stiffness of structures. Therefore, mode shapes are deemed suitable for damage identification in structures.

The investigation of surface damage has been ongoing for several decades. Räsänen, Silvennoinen, Peiponen, and Asakura (1994) examined damage detection on metallic surfaces with slight roughness. They considered computer-produced holograms as sensors for monitoring surface texture and concluded that processing these hologram images could be a powerful tool for identifying surface damage. Zhang, Chang, and Jamshidi (2020) utilized a single-stage detector to identify damage on the surface of concrete bridges. They emphasized that timely and early identification of surface damages is crucial for maintaining the reliability, safety, and

functionality of concrete bridge structures. Erkal and Hajjar (2017) conducted a study on the identification of surface damages based on predicted surface characteristics. This study employed high-resolution 3-D laser scans combined with images to provide geometrical range data. Shihavuddin et al. (2019) investigated surface damage identification in wind turbines using the deep learning method. Inspection images of wind turbines were obtained using drones, and these images were fed into a convolutional neural network for training in damage detection. Hu, Wang, Lee, and Su (2006) presented an investigation on the identification of surface cracks in laminated composite structures based on strain energy and modal analysis. Li, Gao, Guo, He, and Shao (2019) evaluated damage detection of cable surfaces in cable bridges using image mosaicking and optical techniques. Additionally, there have been studies on road damage detection. For example, Shim, Chun, and Ryu (2019) studied damage detection of road surfaces using object recognition based on the Fast R-CNN algorithm.

The wavelet transform is a suitable tool for processing the vibration mode shape of structures. The wavelet transform can be one-dimensional or two-dimensional. It also can be continuous or discrete in terms of continuity. Based on the signal's dimension, the desired type of wavelet transform is selected. So far, many studies have been conducted to localize damages in beam structures using different versions of the wavelet transform. For instance, Rucka (2011) proposed using higher mode shapes in the one-dimensional continuous wavelet transform to detect damages in composite beam structures. This study demonstrated that some low-level damages could only be detected in some higher-mode shapes. Cao, Cheng, Su, and Xu (2012) conducted an experimental study to identify damages in beams using wavelet transform. A multi-scale pseudo-force model was used in the wavelet domain. Findings showed the efficiency of their proposed model in detecting cracks and slot-shape damages. Montanari, Spagnoli, Basu, and Broderick (2015) used the one-dimensional continuous wavelet transform to minimize the desired sampling points required for detecting cracks in beam structures. Also, the wavelet function 'Coif4' was introduced as the most effective function for detecting cracks in beams. Serra and Lopez (2017) investigated damage localization in beam-like structures using the one-dimensional continuous wavelet transform. In the form of a numerical study, they localized damages with a high accuracy. The analyzed signals were mode shapes. Ramesh and Rao (2018) stated that the higher mode shapes are more sensitive to damage in beam structures. Also, similar to the wavelet transform, the modal strain energy was an effective method for damage detection in composite beam structures.

Saadatmorad, Jafari-Talookolaei, Pashaei, Khatir, and Wahab (2022d) proposed a Pearson correlation-based function obtained from the mode shapes. They fed it into the one-dimensional discrete wavelet transform to detect damage in steel beam structures. Findings show that using this function improves the damage detection accuracy compared to the feeding mode shape signal into the wavelet transform. Saadatmorad, Jafari-Talookolaei, Pashaei, Khatir, and Wahab (2022e) suggested a novel scheme to detect damage in plate structures using the two-dimensional discrete wavelet transform and quantify the level of damage using a type of artificial neural network called radial basis function network. Also, in another work, Saadatmorad, Jafari-Talookolaei, Pashaei, and Khatir (2022a) used artificial neural networks to quantify damage levels. Saadatmorad, Jafari-Talookolaei, Pashaei, and Khatir (2022b) used sound signals of damaged composite structures and the one-dimensional continuous wavelet transform to localize damage. Saadatmorad, Jafari-Talookolaei, Pashaei, Khatir, and Wahab (2022f) combined the one-dimensional and two-dimensional to detect damage in plate structures. Liu, Wang, Li, and Yu (2024) used an index called the change of wavelet total energy and another index called the ratio of wavelet energy change as the time-varying damage detection method to identify damage in the

steel beam bridge. Their results showed the efficiency of the indices. The present paper focuses on on-surface damage detection in beam structures using wavelet-based mode shape differences.

2. Finite element formulations

In this study, the Finite Element Method (FEM) is used for numerical modeling of the beam. Based on the Euler-Bernoulli beam theory, a simple element with two end nodes is considered, where each node has two degrees of freedom: deflection and slope. In other words, a simple beam element with four degrees of freedom is considered. By applying the standard process for calculating the stiffness ([K^e]) and mass ([M^e]) matrices of the element, it can be written:

$$[K^e] = \begin{bmatrix} \dfrac{12EI}{l_e^3} & \dfrac{6EI}{l_e^2} & \dfrac{-12EI}{l_e^3} & \dfrac{6EI}{l_e^2} \\ \dfrac{6EI}{l_e^2} & \dfrac{4EI}{l_e} & \dfrac{-6EI}{l_e^2} & \dfrac{2EI}{l_e} \\ \dfrac{-12EI}{l_e^3} & \dfrac{-6EI}{l_e^2} & \dfrac{12EI}{l_e^3} & \dfrac{-6EI}{l_e^2} \\ \dfrac{6EI}{l_e^2} & \dfrac{2EI}{l_e} & \dfrac{-6EI}{l_e^2} & \dfrac{4EI}{l_e} \end{bmatrix} \tag{1}$$

$$[M^e] = \begin{bmatrix} \dfrac{156\rho A l_e}{420} & \dfrac{22\rho A l_e^2}{420} & \dfrac{54\rho A l_e}{420} & \dfrac{-13\rho A l_e^2}{420} \\ \dfrac{22\rho A l_e^2}{420} & \dfrac{4\rho A l_e^3}{420} & \dfrac{13\rho A l_e^2}{420} & \dfrac{-3\rho A l_e^3}{420} \\ \dfrac{54\rho A l_e}{420} & \dfrac{13\rho A l_e^2}{420} & \dfrac{156\rho A l_e}{420} & \dfrac{-22\rho A l_e^2}{420} \\ \dfrac{-13\rho A l_e^2}{420} & \dfrac{-3\rho A l_e^3}{420} & \dfrac{-22\rho A l_e^2}{420} & \dfrac{4\rho A l_e^3}{420} \end{bmatrix} \tag{2}$$

In this context, E represents Young's modulus, I denotes the second moment of area, l_e signifies the element length, ρ stands for density, and A indicates the cross-sectional area.

By assembling the stiffness and mass matrices of each element, the overall stiffness ($[K]$) and mass ($[M]$) matrices of the structure can be derived. The discretized governing equation of motion for a vibrating system has a well-known form as follows (Jafari-Talookolaei, Kargarnovin, & Ahmadian, 2013):

$$[M]\{\ddot{x}(t)\} + [K]\{x(t)\} = 0 \tag{3}$$

Where $\{x(t)\}$ and $\{\ddot{x}(t)\}$ are displacement and acceleration vectors of the discrete beam, respectively. By considering the response $\{x\} = \{\varphi\}e^{i\omega t}$, Equation (3) can be rewritten as follows:

$$([K] - \omega^2[M])\{\varphi\} = 0 \tag{4}$$

Where $\{\varphi\}$ represents the vibration amplitude, ω is the natural frequency, and i is the imaginary unit. Equation (4) employs the standard eigenvalue technique, from which the natural frequencies (eigenvalues) and mode shapes (eigenvectors) can be determined.

3. Proposed method

This paper presents a new method using wavelet transform and subtraction of intact and damaged mode shapes. Figure 1 shows the flowchart of the proposed method in this research. First, the mode shape related to an intact beam is obtained by FEM. For each on-surface damage scenario, the difference between damaged and intact mode shapes is obtained to form the final version of the on-surface damaged mode shape.
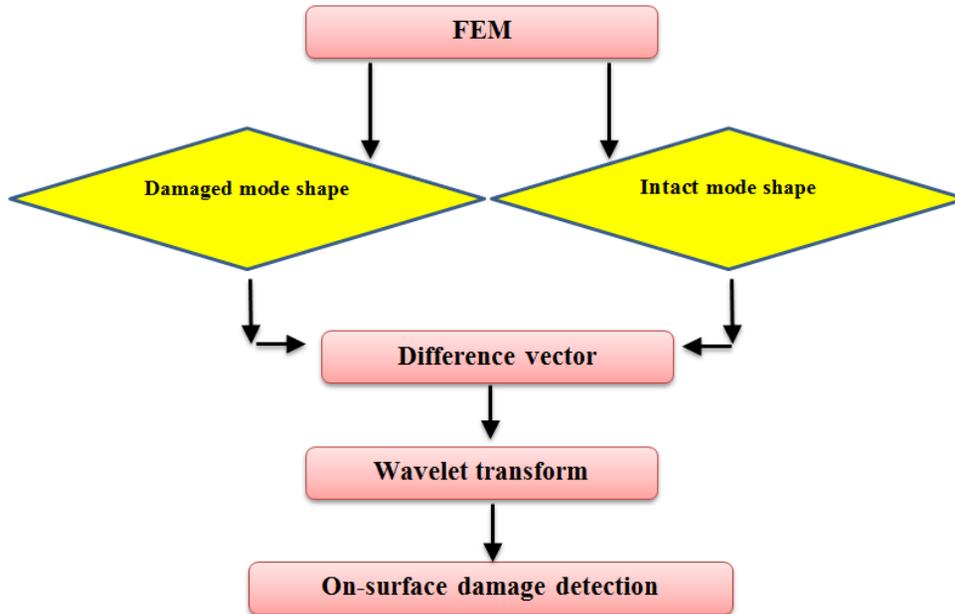
Figure 1. Flowchart of the proposed method in this research

If the damaged mode shape is denoted by w_d and the intact mode shape by w_{intact}, then the difference vector is defined as follows:

$$R = w_d - w_{intact} \tag{5}$$

Given that on-surface damages constitute low-level damage, amplifying local discontinuities can enhance the capability for on-surface damage detection. The difference vector serves to magnify local discontinuities within the mode-shape data samples. Upon converting the data samples to the new format, a continuous wavelet transform is employed, as expressed in the following equation (Abdulkareem et al., 2021):

$$C(u,s) = \langle R(X), \psi(X)_{u,s} \rangle = \frac{1}{\sqrt{s}} \int_{-\infty}^{+\infty} R(X) \psi\left(\frac{x-u}{s}\right) dX \tag{6}$$

Where X shows the space variable of the difference vector of mode shape R(X), u is the shifting parameter, and s denotes the scale parameter. $\psi(X)_{u,s}$ is the wavelet function, $C(u,s)$ shows the wavelet coefficients.

Due to the inherent sensitivity of wavelet transform to tiny local jumps in signals, increasing the amount of the tiny local jumps, it is expected that the ability of on-surface damage detection to be enhanced.

Note that the following conditions have to be satisfied for a wavelet function:

$$\int_{-\infty}^{+\infty} |\psi(X)|^2 \, dX < \infty \tag{7}$$

Another property of wavelet functions is that their Fourier transform does not contain a zero frequency component, thus:

$$\int_{-\infty}^{+\infty} \frac{\left| \frac{1}{\sqrt{2\pi}} \int \psi(X) e^{iz\omega} \, dX \right|^2}{|\omega|} \, dw < \infty \tag{8}$$

Where i is $\sqrt{-1}$, and ω indicates the wavelet function's central frequency. Note that the above condition of wavelet functions is named the admissibility condition. The admissibility condition means that in z space, the average of the wavelet function is zero, therefore:

$$\int_{-\infty}^{+\infty} \psi(X) \, dx = 0 \tag{9}$$

4. Results

In this section, numerical and experimental results are presented. The evaluation commences with the numerical scenarios, followed by the experimental scenarios. Table 1 enumerates the single and multiple damage scenarios that were considered in the numerical investigation. It should be noted that on-surface or on-coating damages are classified as low-level damages, with the damage levels designated as equal to or below 10% in Table 1.

Figure 2 graphically illustrates the on-surface damage scenarios as tabulated in Table 1. To model these on-surface damages, the following expression is utilized (Saadatmorad et al., 2021):

$$[K^e]_d = \alpha[K^e] \tag{10-a}$$

$$D = \frac{[K^e] - [K^e]_d}{[Ke]} \times 100 = \frac{[K^e] - \alpha[K^e]}{[Ke]} \times 100 = (1 - \alpha) \times 100 \tag{10-b}$$

Where D is the damage level, $\mathrm{K}ed$ is the stiffness of the damage element, and α is a constant $(0 < \alpha < 1)$.

In other words, after programming based on the Finite Element Method (FEM) for an intact beam, damage is applied to the structure by reducing the damage element stiffness matrix. The mode shapes obtained from this methodology are our damaged mode shape signals.

Scenario 1

Scenario 2

Scenario 3

Scenario 4

Scenario 5
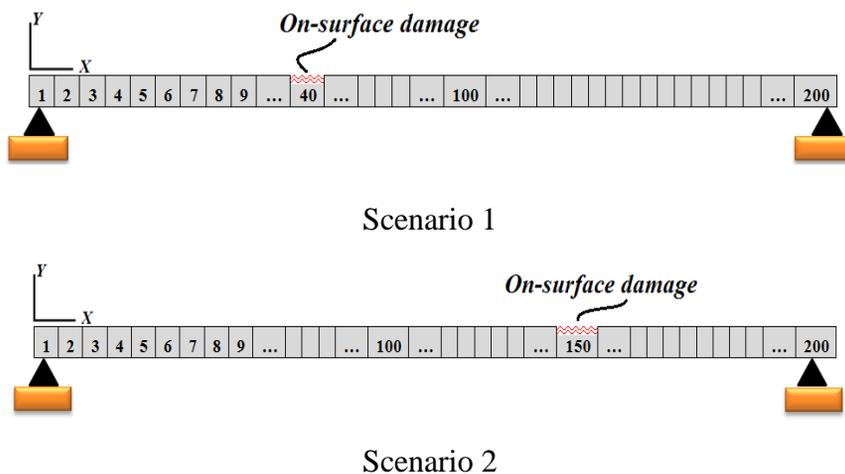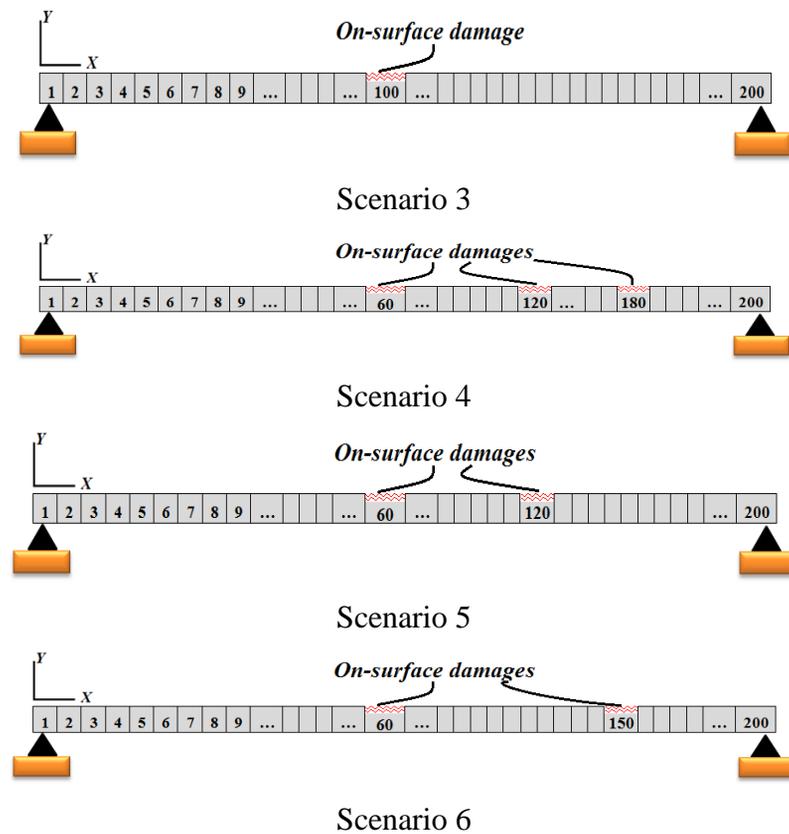
Scenario 6

Figure 2. On-surface damages scenarios for the numerical investigations

**Table 1**

Damage scenarios for the numerical investigation

Scenario number	On-surface damage location	Damage level
Scenario 1	40	10%
Scenario 2	150	7%
Scenario 3	100	5%
Scenario 4	60, 120, 180	7%, 5%, 10%
Scenario 5	60, 120	6%, 4%
Scenario 6	60, 150	8%, 8%

As seen in Figure 2 and Table 1, three on-surface damage scenarios are examined in our numerical investigation. The 40th element is damaged in the first scenario, and the damage level is 10%. The 150th element is damaged in the second scenario, and the damage level is 7%. In the third scenario, the 100th element is damaged, and the damage level is 5%. Also, multiple damage scenarios are considered in the scenarios from 4 to 6.
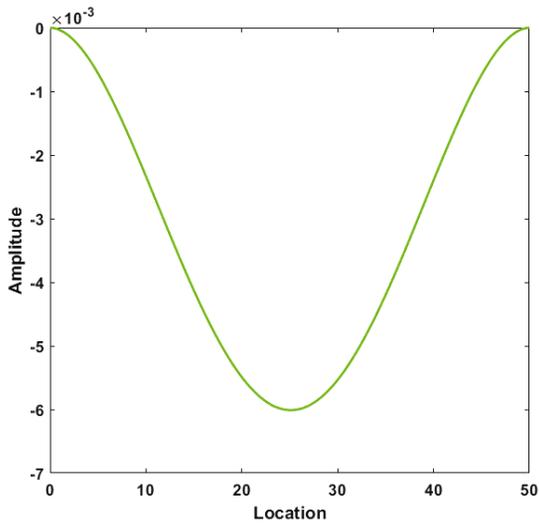
Figure 2 depicts damage mode shapes corresponding to the six considered damage scenarios. Figures 4, 5, and 6 show the obtained results by the proposed method for Scenarios 1, 2, and 3, respectively. The peak of the wavelet coefficient (C) shows the location of the damage. According to Figure 4, the maximum wavelet coefficient is located at the location X = 40. Thus, it means that the on-surface damage related to Scenario 1 is detected with high accuracy.
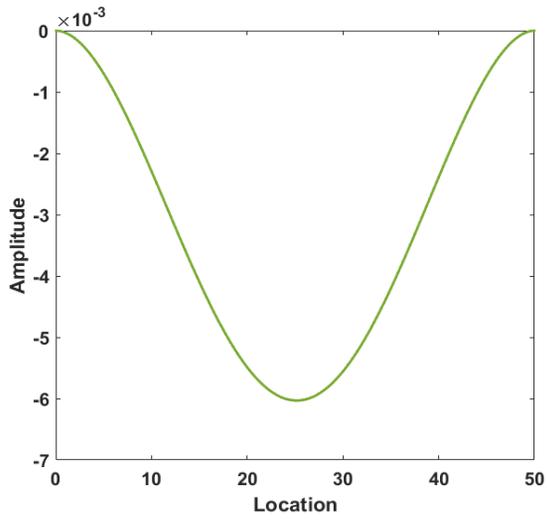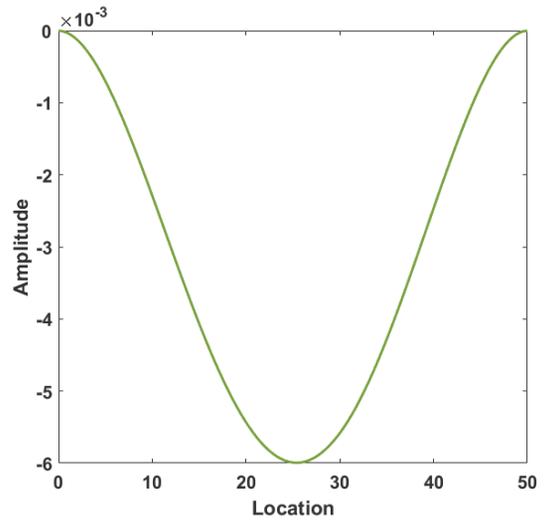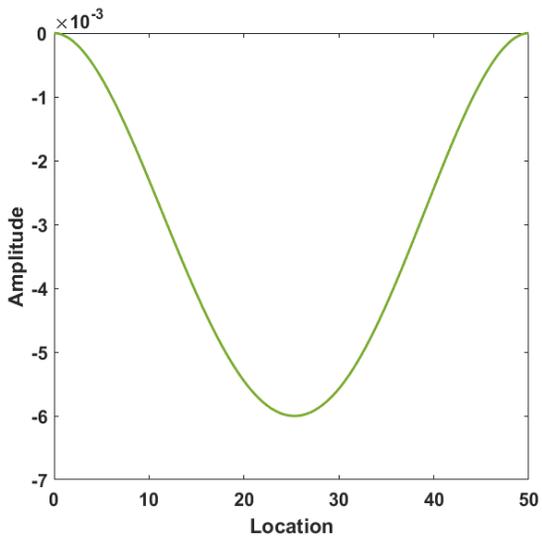
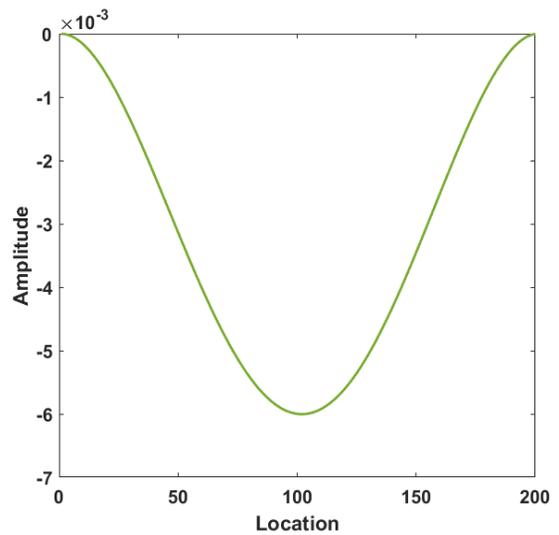Mode shape of scenario 1
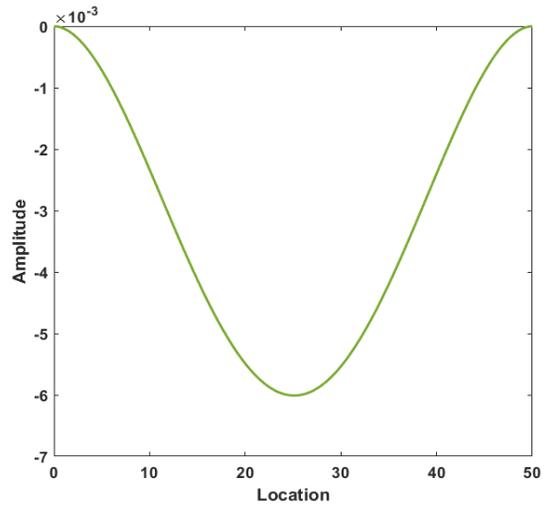
Mode shape of scenario 2
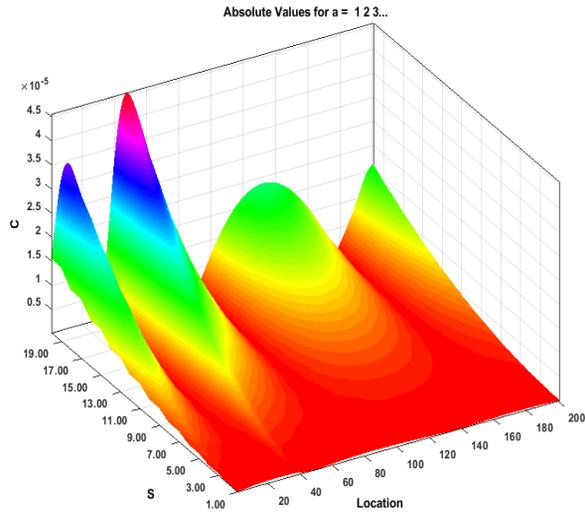
Mode shape of scenario 3

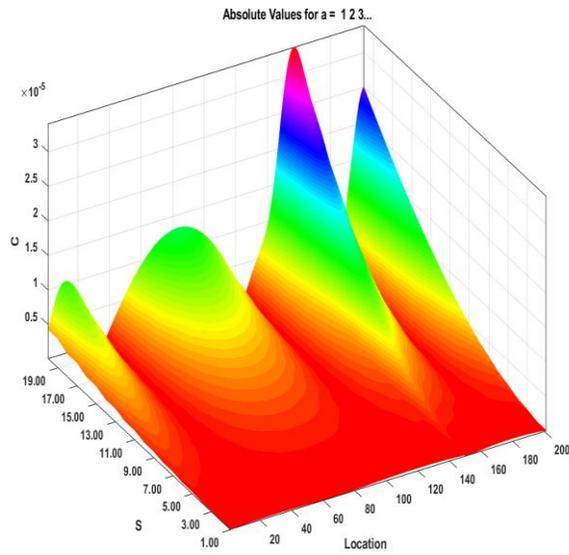Mode shape of scenario 4

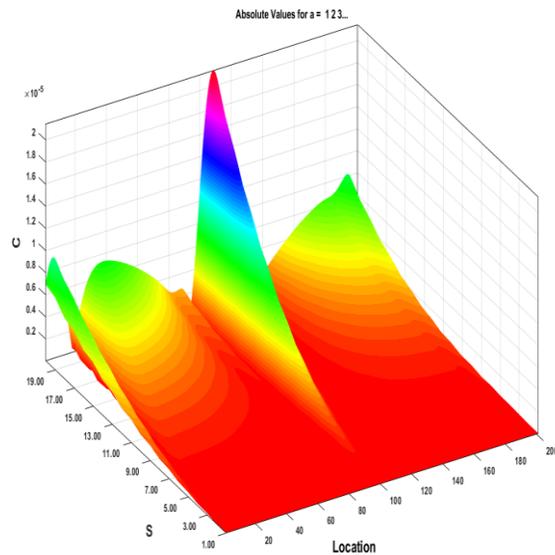Mode shape of scenario 5

Mode shape of scenario 6

Figure 3. Damage mode shapes corresponding to the six considered damage scenarios

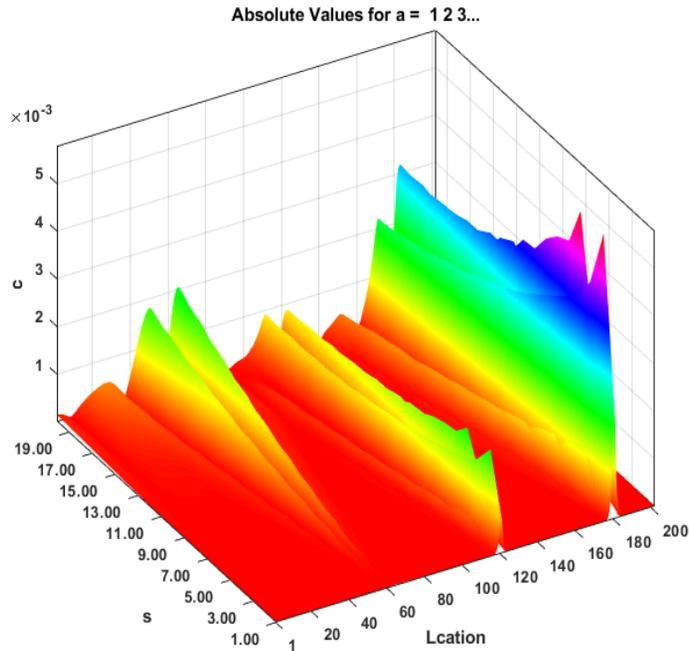**Figure 4.** The obtained result by the proposed method for Scenario 1

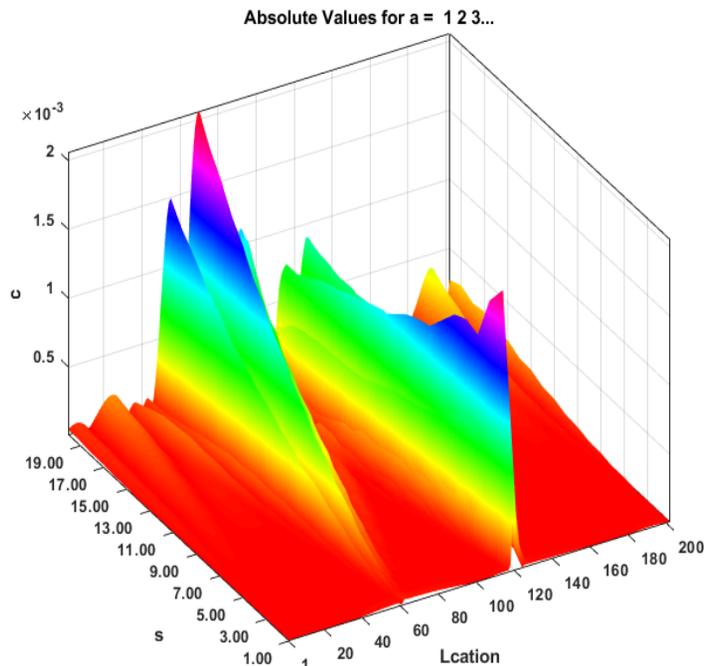**Figure 5.** The obtained result by the proposed method for Scenario 2

Figure 6. The obtained result by the proposed method for Scenario 3

Figure 5 indicates that the maximum wavelet coefficient is located at X = 150. Thus, it means that the on-surface damage related to Scenario 2 is also detected with high accuracy. Finally, Figure 6 indicates that the maximum wavelet coefficient is located at X = 100. Consequently, it means that the on-surface damage related to Scenario 3 is also detected with high precision.
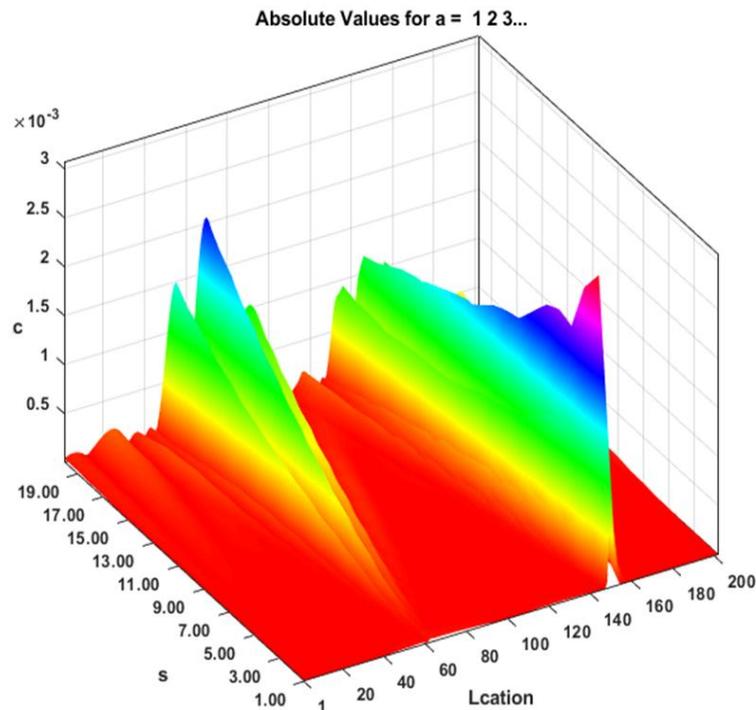

Figure 7. The obtained result by the proposed method for Scenario 4

The first multiple damages in scenario 4 are detected with high accuracy, according to Figure 7.

**Figure 8.** The obtained result by the proposed method for Scenario 5

Also, the second multiple damages in scenario 5 are detected with high accuracy, according to Figure 8.

**Figure 9.** The obtained result by the proposed method for Scenario 6

Finally, the third multiple damage in scenario 6 is detected with high accuracy, according to Figure 9. According to the results mentioned above, it is proved that our proposed method provides a high-accuracy tool for detecting very low-level damages that occur on the surface of beam structures. However, in order to verify its accuracy in practical and industrial applications, an experimental investigation is conducted. In this way, a steel beam shown in Figure 10 is used to be tested. The length of the beam is divided into ten equal elements, and each element is numbered, as seen in Figure 11. For every ten points, the experimental intact and damaged mode shapes are obtained to acquire data to evaluate the performance of the proposed method in real-world on-surface damage scenarios. On-surface damage is created on the beam by the CNC milling machine as can be seen in Figure 10. A soft clamp supports the beam to simulate free-free boundary conditions. A DJB A120V accelerometer is employed to measure acceleration. The accelerometer is mounted at point 4 of the beam. An 8202BK hammer equipped with an 8200BK dynamometer is utilized to apply force to the beam. A 2647A amplifier is also utilized to transform the power signal. The accelerometer is fixed at point 4, and at all points, the impact force is applied via the hammer. This experiment is conducted once for the intact beam and once for the on-surface damaged beam.

Figure 11 indicates the experimental results of the current study. As can be seen in this figure, the maximum wavelet coefficient is located between $X = 7$ and $X = 8$. Thus, it means that the on-surface damage related to Scenario 1 is detected with high accuracy.
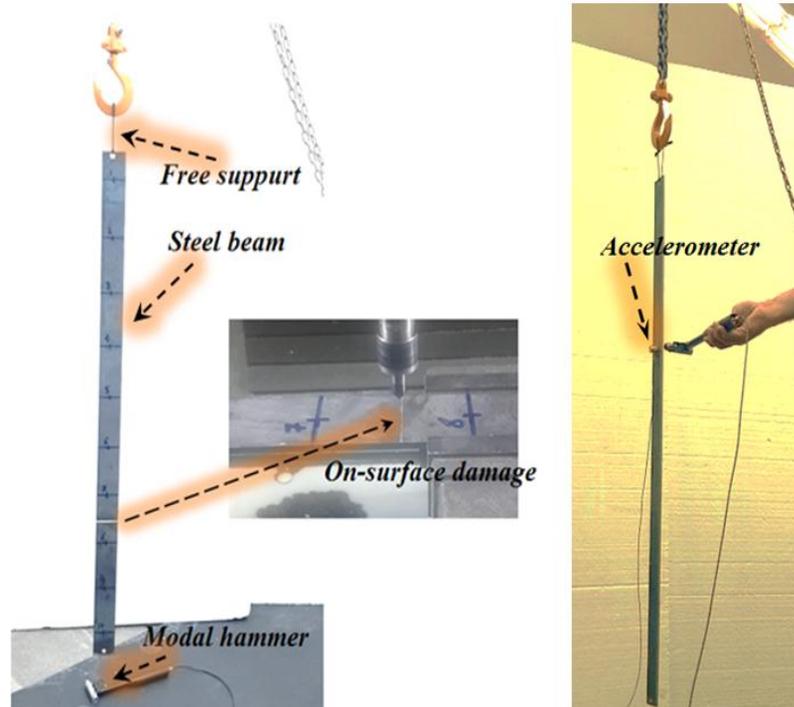
Figure 10. Left: experimental setup of this study; Right: modal impact hammer testing

As seen in Figure 10, the damage can be detected with high accuracy in experimental analysis using the proposed method. However, the damage can be seen by the eyes, and the main limitation in mode shape-based damage detection is the provision of the desired sampling points. Thus, acquiring many empirical mode shape sampling points is time-consuming. Therefore, it is necessary to provide equipment to record the empirical mode shape by numerous sampling points faster in the future.
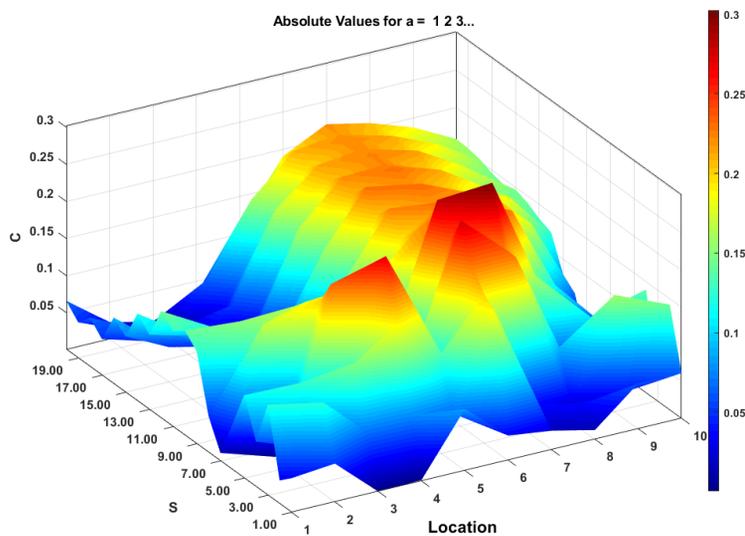
Figure 11. The obtained result from the experimental investigation

5. Conclusions

This research presents a new and sensitive method to detect damage on beam's surfaces. In this way, using the finite element method, a numerical model of the beam is created to obtain the intact and damaged mode shapes. The type of modeled damage is on-surface damages (i.e., damages with a level below 10%). Wavelet transform is usually unable to detect damages below

10%. Our proposed method creates a vector of mode shapes by subtracting the intact signals from on-surface damaged signals. Then, the vector obtained is used in the one-dimensional continuous wavelet transform. This procedure creates a robust tool to detect slight damages. The results of the numerical study demonstrate that on-surface damages can be detected ideally. Also, experimental investigation verifies the efficiency of the proposed method for practical applications.

References

Abdulkareem, M., Bakhary, N., Ganiyu, A., Nathaniel, O., Jassam, T. M., & Al-Mansob, R. A. (2021). Consideration of uncertainty in damage detection using interval analysis wavelet without baseline data. *Journal of Structural Integrity and Maintenance, 6*(2), 99-109.

Azami, M., & Salehi, M. (2019). Response-based multiple structural damage localization through multi-channel empirical mode decomposition. *Journal of Structural Integrity and Maintenance, 4*(4), 195-206.

Bjørheim, F., Siriwardane, S. C., & Pavlou, D. (2022). A review of fatigue damage detection and measurement techniques. *International Journal of Fatigue, 154*, Article 106556.

Cao, M., Cheng, L., Su, Z., & Xu, H. (2012). A multi-scale pseudo-force model in wavelet domain for identification of damage in structural components. *Mechanical Systems and Signal Processing, 28*, 638-659.

Erkal, B. G., & Hajjar, J. F. (2017). Laser-based surface damage detection and quantification using predicted surface properties. *Automation in Construction, 83*, 285-302.

Hu, H., Wang, B. T., Lee, C. H., & Su, J. S. (2006). Damage detection of surface cracks in composite laminates using modal analysis and strain energy method. *Composite Structures, 74*(4), 399-405.

Jafari-Talookolaei, R.-A., Kargarnovin, M. H., & Ahmadian, M. T. (2013). Dynamic response of a delaminated composite beam with general lay-ups based on the first-order shear deformation theory. *Composites Part B: Engineering, 55*, 65-78,

Khatir, S., Dekemele, K., Loccufier, M., Khatir, T., & Wahab, M. A. (2018). Crack identification method in beam-like structures using changes in experimentally measured frequencies and Particle Swarm Optimization. *Comptes Rendus Mécanique, 346*(2), 110-120.

Li, X., Gao, C., Guo, Y., He, F., & Shao, Y. (2019). Cable surface damage detection in cable-stayed bridges using optical techniques and image mosaicking. *Optics & Laser Technology, 110*, 36-43.

Liu, J. L., Wang, S. F., Li, Y. Z., & Yu, A. H. (2024). Time-varying damage detection in beam structures using variational mode decomposition and continuous wavelet transform. *Construction and Building Materials, 411*, Article 134416.

McGeown, C., Huseynov, F., Hester, D., McGetrick, P., Obrien, E. J., & Pakrashi, V. (2021). Using measured rotation on a beam to detect changes in its structural condition. *Journal of Structural Integrity and Maintenance, 6*(3), 159-166.

Montanari, L., Spagnoli, A., Basu, B., & Broderick, B. (2015). On the effect of spatial sampling in damage detection of cracked beams by continuous wavelet transform. *Journal of Sound and Vibration, 345*, 233-249.

Ramesh, L., & Rao, P. S. (2018). Damage detection in structural beams using model strain energy method and wavelet transform approach. *Materials Today: Proceedings, 5*(9), 19565-19575.

Räsänen, J., Silvennoinen, R., Peiponen, K. E., & Asakura, T. (1994). On surface damage detection of slightly rough metal surfaces. *Optics and Lasers in Engineering, 20*(1), 65-69.

Rucka, M. (2011). Damage detection in beams using wavelet transform on higher vibration modes. *Journal of Theoretical and Applied Mechanics, 49*(2), 399-417.

Saadatmorad, M., Jafari-Talookolaei, R.-A., Pashaei, M. H., & Khatir, S. (2021). Damage detection on rectangular laminated composite plates using wavelet based convolutional neural network technique. *Composite Structures, 278*, Article 114656.

Saadatmorad, M., Jafari-Talookolaei, R.-A., Pashaei, M. H., & Khatir, S. (2022a). Damage detection in rectangular laminated composite plate structures using a combination of wavelet transforms and artificial neural networks. *Journal of Vibration Engineering & Technologies, 10*(5), 1647-1664.

Saadatmorad, M., Jafari-Talookolaei, R.-A., Pashaei, M. H., & Khatir, S. (2022b). Experimental acoustic-wavelet method for damage detection on laminated composite structures. In *International conference of steel and composite for engineering structures* (pp. 93-113). Cham, Switzerland: Springer International Publishing.

Saadatmorad, M., Jafari-Talookolaei, R.-A., Pashaei, M. H., Khatir, S., & Wahab, M. A. (2022c). Application of multilayer perceptron neural network for damage detection in rectangular laminated composite plates based on vibrational analysis. In *Proceedings of the 2nd international conference on structural damage modelling and assessment* (pp. 163-178). Singapore: Springer.

Saadatmorad, M., Jafari-Talookolaei, R.-A., Pashaei, M. H., Khatir, S., & Wahab, M. A. (2022d). Pearson correlation and discrete wavelet transform for crack identification in steel beams. *Mathematics, 10*(15), Article 2689.

Saadatmorad, M., Jafari-Talookolaei, R.-A., Pashaei, M. H., Khatir, S., & Wahab, M. A. (2022e). A robust technique for damage identification of marine fiberglass rectangular composite plates using 2-D discrete wavelet transform and radial basis function networks. *Ocean Engineering, 263*, Article 112317.

Saadatmorad, M., Jafari-Talookolaei, R.-A., Pashaei, M. H., Khatir, S., & Wahab, M. A. (2022f). Delamination detection of rectangular laminated composite plates by combining the one-dimensional and two-dimensional discrete wavelet transforms. In *Proceedings of the 10th international conference on fracture fatigue and wear: FFW 2022, 2-3 August, Ghent University, Belgium* (pp. 41-51). Singapore: Springer Nature.

Saadatmorad, M., Khatir, S., Le, C. T., Benaissa, B., & Mahmoudi, S. (2024). Detecting damages in metallic beam structures using a novel wavelet selection criterion. *Journal of Sound and Vibration, 578*, Article 118297.

Saadatmorad, M., Shahavi, M. H., & Gholipour, A. (2024). Damage detection in laminated composite beams reinforced with nano-particles using covariance of vibration mode shape and wavelet transform. *Journal of Vibration Engineering & Technologies, 12*(3), 2865-2875.

Saadatmorad, M., Siavashi, M., Jafari-Talookolaei, R.-A., Pashaei, M. H., Khatir, S., & Le, C. T. (2021). Multilayer perceptron neural network for damage identification based on dynamic analysis. In *Structural health monitoring and engineering structures* (pp. 29-48). Singapore: Springer.

Serra, R., & Lopez, L. (2017). Damage detection methodology on beam-like structures based on combined modal Wavelet Transform strategy. *Mechanics & Industry, 18*(8), Article 807.

Shihavuddin, A. S. M., Chen, X., Fedorov, V., Christensen, A. N., Riis, N. A. B., Branner, K., … Paulsen, R. R. (2019). Wind turbine surface damage detection by deep learning aided drone inspection analysis. *Energies, 12*(4), Article 676.

Shim, S., Chun, C., & Ryu, S. K. (2019). Road surface damage detection based on object recognition using Fast R-CNN. *The Journal of the Korea Institute of Intelligent Transport Systems, 18*(2), 104-113.

Wahab, M. A., & De Roeck, G. (1999). Damage detection in bridges using modal curvatures: Application to a real damage scenario. *Journal of Sound and Vibration, 226*(2), 217-235.

Zhang, C., Chang, C. C., & Jamshidi, M. (2020). Concrete bridge surface damage detection using a single-stage detector. *Computer-Aided Civil and Infrastructure Engineering, 35*(4), 389-409.